

# **Development of PP Catalysts and PP Manufacturing Processes**

AKINOBU SHIGA

*LUMMOX Research Laboratory*

[aas55@mail2.accsnet.ne.jp](mailto:aas55@mail2.accsnet.ne.jp)

## **ABSTRACT**

Isotactic polypropylene(PP) is one of the most useful plastics for modern human life. Saving energy and resources is the most important issue of the PP production. Nowadays, PP is mainly produced by gas phase process with sophisticated heterogeneous catalysts in industry. First, the history of development of PP manufacturing processes: 1st generation solvent polymerization process, the 2<sup>nd</sup> generation non-deashing process and the 3<sup>rd</sup> generation gas polymerization process, is briefly reviewed. Second, preparation of heterogeneous polymerization catalysts and studies of polymerization mechanism are described. It is important for catalyst development getting rational working hypotheses. Simulation of polymerization based on an atomistic modeling of active sites is a powerful tool to do so. Finally, cluster model approach for clarifying roles of donor compounds in MgCl<sub>2</sub> supported catalysts is presented.

## **1. INTRODUCTION**

One of the most important discoveries in chemistry and in chemical industries in the last century is the Ziegler-Natta catalysts for polymerization of olefin. World consumption of polyolefins, high-density polyethylene(HDPE), linear low-density polyethylene(LLDPE) and polypropylene(PP), was greater than 70 million tons in 2006 and will be markedly increasing in this century. The saving of the consumption of energies and raw materials of the production is the most important and urgent issue.

The manufacturing process of PP is classified into several types, so called the first generation process, the second generation process and the third generation process.

The highly active heterogeneous catalysts have modernized the manufacturing process of polyolefin and nowadays, gas phase process (the third generation process) is the main stream of PP production process. The cost of plant construction and the consumption of raw materials and utilities have been drastically reduced by employing gas phase process. Hence, gas phase process is one of the typical examples of so-called “green process”. High mileage polymerization catalyst is a key technology for

realization of the green process. In addition, the needs of the catalysts which enable to control molecular weight of polymers and its distribution, copolymerization ratio, regio- and stereoselectivities and so on, are more increasing to produce polymers with desirable chemical and physical properties.

It is difficult to develop such sophisticated catalysts only by means of trial and error bases. One has to clarify the relationship between the structure of the active site and the catalyst performance on the basis of the precise and quantitative understanding of polymerization mechanism.

## 2. POLYMERIZATION MECHANISM OF NATTA CATALYSTS

### 2.1 Kinetic study of propylene polymerization with $\alpha$ -TiCl<sub>3</sub>/Al(C<sub>2</sub>H<sub>5</sub>)<sub>3</sub>

According to Natta [3], the polymerization rate under steady-state conditions is given by Equation (1);

$$R_p = A \exp^{-E/RT} P_{C_3H_6} G_{Ti} \quad (1)$$

where,  $R_p$  = rate of polymerization (g.PP/hr),  $A = 10^{7.3}$ ,  $E = 10$  kcal/mol,  $T = K$ ,  
 $P_{C_3H_6}$  = partial pressure of propylene (atm.),  
 $G_{Ti}$  = g. of TiCl<sub>3</sub> in the catalytic system.

The rate is independent of the Al(C<sub>2</sub>H<sub>5</sub>)<sub>3</sub> concentration. The mechanism of chain termination has been investigated by adding radioactive aluminum alkyl labeled by C<sup>14</sup>, followed by the analysis of the radioactive assay of the polymer. The relation between the factor affecting the intrinsic viscosity of the mainly isotactic PP fraction and inverse of the degree of polymerization,  $1/P_n$ , is given by Equation (2);

$$1/P_n = (k_1 + k_2 P_{C_3H_6} + k_3 (C_{Al})^{1/2} + k_4 P_{C_3H_6} G_{Ti}) / (k_p P_{C_3H_6}) \quad (2)$$

where,  $k_1$ ,  $k_2$ ,  $k_3$  and  $k_4$  stand for the rate constants of the different chain-breaking processes causing termination,  $k_p$  is the propagation rate constant, and  $C_{Al}$  is the aluminum alkyl concentration.

### 2.2 Structure of TiCl<sub>3</sub>

#### *Crystalline modifications of TiCl<sub>3</sub>*

Natta discovered that the crystal structure of TiCl<sub>3</sub> has an essential role on stereospecific polymerization of propylene. According to Natta et al. [4], there are four crystalline modifications of TiCl<sub>3</sub>: the  $\alpha$ -,  $\gamma$ -,  $\delta$ -forms (violet) and the  $\beta$ -form (brown).

Violet TiCl<sub>3</sub> having a layer structure, gives highly isotactic PP, whereas  $\beta$ -TiCl<sub>3</sub> having

a fiber-shaped structure, gives atactic PP in a very low yield. The difference in these three forms of violet  $\text{TiCl}_3$  is found only in the mode of stacking of the common bidimensional  $\text{TiCl}_3$  sheets (layer structures). The  $\alpha$ -form of  $\text{TiCl}_3$  is specified by the layers that has a hexagonal close-packing of the chlorine atoms (AB,AB...). The  $\gamma$ -form of  $\text{TiCl}_3$  has a cubic close-packing of the chlorine atoms (ABC,ABC...). In the case of  $\delta$ - $\text{TiCl}_3$ , the mode of stacking of the structural layers is given by some statistical average of the modes of packing in the  $\alpha$ - and  $\gamma$ -forms. The  $\delta$ -form  $\text{TiCl}_3$  is obtained by grinding of  $\alpha$ - or  $\gamma$ -  $\text{TiCl}_3$ .

#### ***Effect of the specific surface area of $\delta$ - $\text{TiCl}_3$***

$\delta$ - $\text{TiCl}_3$  is used in PP production because of its high catalytic activity for polymerization [5]. Keii et al. [6] examined the effect of grinding of  $\alpha$ - $\text{TiCl}_3$  on propylene polymerization in detail and revealed that the rate of propagation was proportional to the specific surface area of the  $\text{TiCl}_3$  under steady-state condition, provided that the "true" specific surface area was evaluated by treating the  $\text{TiCl}_3$  with solvent to de-agglomerate.

### **2.3 Morphology of Catalyst Particles and As polymerized Polymer Particles**

Many morphological studies on the structure of  $\delta$ - $\text{TiCl}_3$  catalyst particles and as polymerized polymer particles have revealed that  $\delta$ - $\text{TiCl}_3$  catalysts used in industry are in the forms of 10-30 $\mu$  particles consisting of loosely bound agglomerates of fine  $\text{TiCl}_3$  crystallines, several tens to several hundreds of angstrom in diameter [7],[8]. As shown in Fig. 1, Rodoriguez et al. [9] observed the first direct evidence that the polymerization took place on the surface

of  $\text{TiCl}_3$  crystallines by transmission electron microscopy. According to Kakugo et al. [10], polymer particles of PP are tertiary particles consisting of secondary polymer particles of the diameter of about 1 $\mu$  and of primary polymer particles of some tens smaller than the secondary particles, each of which has grown on the same  $\text{TiCl}_3$  crystalline

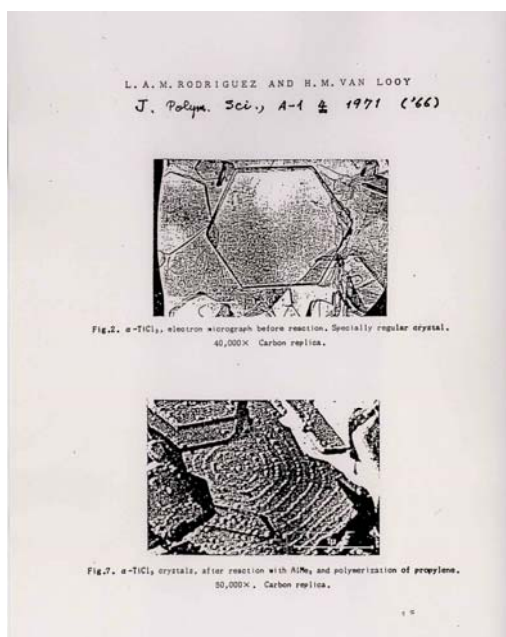


Fig. 1 TEM of  $\alpha$ -TiCl<sub>3</sub> single crystals

## 2.4 Stereochemistry of Polymers

The fraction(%) of polymer, which is not extracted in boiling n-heptane, is used as practical and convenient index of the stereoregularity of PP. However it gives little information on the polymerization mechanism. In the following, we attempt to elucidate the mechanism of determining the region- and stereo-selectivity of propylene polymerization.

There are four modes of chain connectivity in  $\alpha$ -olefin polymerization : head to tail, tail to head, head to head and tail to tail. The head to head or tail to tail connection which can be detected by IR spectroscopy [11], is not able to yield a highly isotactic fraction of PP. Takegami et al. [12] reported that a primary alkyl-metal bond was formed predominantly in the insertion product of an  $\alpha$ -olefin into metal ethyl bonds of the violet TiCl<sub>3</sub>/Al(C<sub>2</sub>H<sub>5</sub>)<sub>3</sub> catalyst.

Cis-opening of an olefinic double bond was first reported by Miyazawa et al. [13] based on the IR analysis of the poly(propylene-1d<sub>1</sub>). Zambelli et al. [14] concluded that cis opening of the double bond and primary insertion took place in the propagation stage from an analysis of the structure of isotactic polymers of cis and trans 1-d<sub>1</sub> propylene and of syndiotactic copolymers of d<sub>6</sub>-propylene with cis and trans 1-d<sub>1</sub> propylene, by NMR spectroscopy.

IsotacticPP has the ...m m m...stereoselectivity. <sup>13</sup>C-FTNMR technique makes it possible to determine the stereoselectivity of the polymer chain [15], [16]. The disorder

in stereoselectivity of the chain provides useful information of the mechanism of determining the stereoselection. Kakugo et al [17] reported that the mmrr, mrrm and mmmr type of disorders were observed in the isotactic fraction of PP obtained with  $\delta$ -TiCl<sub>3</sub> or MgCl<sub>2</sub> supported catalysts, however the mrrm type of disorder was not observed. The possibility of catalytic control of the stereoselection was suggested.

## **2.5 Location of the Active Site on the TiCl<sub>3</sub> Crystalline Surface**

Wilchinsky et al. [18] reported that the crystalline size reduction as calculated from the broadening of X-ray diffraction peaks, representing the direction parallel (300) and transverse (003) to the hexagonal crystal axis, occurred during the grinding of a layer-structure type TiCl<sub>3</sub>. They observed a linear relationship between the catalytic activity and the reciprocal of the crystalline dimensions ( $1/D_{300}$  and  $1/D_{003}$ ). Unfortunately their samples had  $D_{300}/D_{003}$  ratio close to unity and, hence, it was impossible to assign the location of the active sites. We succeeded to obtain  $\delta$ -TiCl<sub>3</sub> catalysts with the varying  $D_{300}/D_{003}$  ratios [19]. The linear relation between the catalytic activity vs.  $1/D_{300}$  and  $1/D_{003}$  in the  $\delta$ -TiCl<sub>3</sub> catalysts. From this result, we deduce that the active sites are located on the edge of the basal faces of the TiCl<sub>3</sub> crystallines.

## **3. ATOMISTIC SIMULATION OF ACTIVE SITES**

An atomistic simulation is one of the powerful method for getting rational working hypotheses of catalyst development.

### **3.1 Cossee Mechanism**

The Cossee mechanism has been widely accepted for the Ziegler-Natta polymerization mechanism as the most plausible [20]. The mechanism is as follows; the active site is a metal alkyl, the olefin coordinates to the vacancy of the metal alkyl to form a  $\pi$ -complex, then the olefin inserts into the metal-alkyl bond through a four-members cyclic transition state, and these procedures are repeated. Kawamura et al. [21] first studied the mechanism of the insertion of ethylene and propylene into  $[\text{Cl}_2\text{TiCH}_3]^+$  by using RHF calculation with DPUMP2 level correction and determined the structures and energies of the reactant, the  $\pi$ -complex, the transition states and the product.

### 3.2 Elucidation an Active Site Model

From the results described in the chapter 2, the active site is specified as follows : A precursor of an active site is located on the edge of the basal face of violet  $\text{TiCl}_3$  crystalline surfaces. The precursor has Cl vacancy and a dangling bonded Cl atom which will be alkylated by an alkylaluminum co-catalyst to form the active site. These are schematically illustrated in Fig. 2.

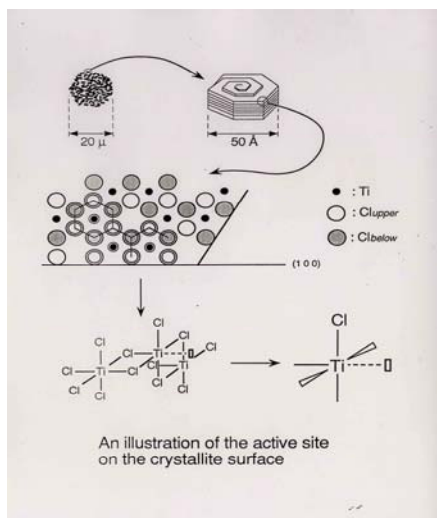


Fig. 2 An illustration of the active site model

### 3.3 PIO Calculations

The paired interacting orbital (PIO) calculation proposed by Fujimoto et al. [22] is a method for unequivocally determining the orbitals which should play dominant roles in chemical interactions between two systems, [A] and [B], which construct a combined system [C]. In the case of the propylene insertion, [C] is the propylene alkyl-titanium complex, while [A] is the alkyl-titanium portion and [B] is the propylene portion. The geometries of [A] and [B] are the same as those in the complex [C] ( $[A-B] \equiv [C]$ ).

The extended Hückel MOs of [A], [B] and [C] are calculated. PIOs are obtained by applying the procedure that was proposed by Fujimoto et al. [22]. It is summarized in the Appendix..

## 4. PROPYLENE INSERTION ON THE SURFACE OF $\text{TiCl}_3$ AND $\text{MgCl}_2$ CRYSTALLINE

We already reported PIO analysis of olefin insertion on the surface of  $\text{TiCl}_3$  crystalline [23]. Here, we compare propylene insertion on  $\text{TiCl}_3$  surface with that on  $\text{MgCl}_2$  supported catalysts surface, and clarify a role of donor compounds in  $\text{MgCl}_2$  supported catalysts. We use 2-methylbutyl-Ti chloride cluster models for active sites on  $\text{TiCl}_3$  or  $\text{MgCl}_2$  crystalline, and di-methyl ether ( $\text{Me}_2\text{O}$ ) as a model of donor compound.

### 4.1 Models

We employed following seven models;

[Oh-d<sup>1</sup>-2MeBuTiCl<sub>2</sub>(MgCl<sub>2</sub>)<sub>3</sub>]/(C<sub>3</sub>H<sub>6</sub>):**(10)** is a model on the MgCl<sub>2</sub>(110) surface,  
[pseudoOh(1)-d<sup>1</sup>-2MeBuTiCl<sub>2</sub>(MgCl<sub>2</sub>)<sub>3</sub>]/(C<sub>3</sub>H<sub>6</sub>):**(11)** is a model on the MgCl<sub>2</sub>(110) surface and has one Cl vacancy at the trans position to the propylene,  
[pseudoOh(2)-d<sup>1</sup>-2MeBuTiCl<sub>2</sub>(MgCl<sub>2</sub>)<sub>3</sub>]/(C<sub>3</sub>H<sub>6</sub>):**(12)** is a model on the MgCl<sub>2</sub>(110) surface and has one Cl vacancy at the trans position to the 2MeBu group,  
[Td-d<sup>1</sup>-2MeBuTiCl<sub>2</sub>(MgCl<sub>2</sub>)<sub>3</sub>]/(C<sub>3</sub>H<sub>6</sub>):**(13)** is a model on the MgCl<sub>2</sub>(100) surface,  
[Oh-d<sup>1</sup>-2MeBuTi<sub>4</sub>Cl<sub>11</sub>]/(C<sub>3</sub>H<sub>6</sub>):**(14)** is a model on the edge of TiCl<sub>3</sub>(003) surface,  
[Oh-d<sup>1</sup>-2MeBuTiCl<sub>2</sub>(Me<sub>2</sub>O)(MgCl<sub>2</sub>)<sub>3</sub>]/(C<sub>3</sub>H<sub>6</sub>):**(15)** is a model on the MgCl<sub>2</sub>(110) surface and has one Me<sub>2</sub>O at the trans position to the propylene,  
[Oh-d<sup>1</sup>-2MeBuTiCl<sub>2</sub>(Me<sub>2</sub>O)<sub>2</sub>(MgCl<sub>2</sub>)<sub>3</sub>]/(C<sub>3</sub>H<sub>6</sub>):**(16)** is a model on the MgCl<sub>2</sub>(100) surface and has two Me<sub>2</sub>O, one of Me<sub>2</sub>O occupies at the trans position to the propylene and the other Me<sub>2</sub>O occupies at the position to the 2MeBu group.

We execute PIO analysis of each model of an intermediate state of propylene insertion into 2-methylbutyl–Ti bond on Cossee mechanism. The model**(10)**, **(11)**, **(12)**, **(13)**, and **(14)** are shown in Fig. 3.

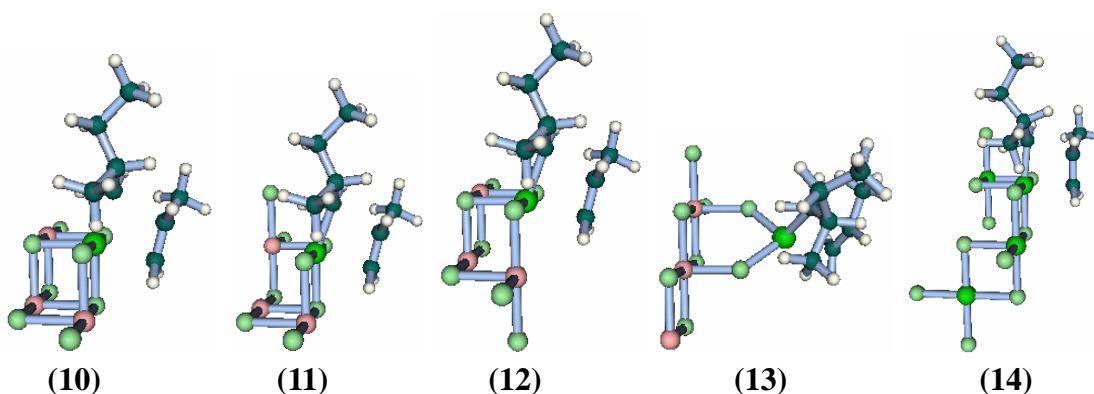


Fig. 3 3D-structures of model**(10)**, **(11)**, **(12)**, **(13)**,and **(14)**

## 4.2 Results and Discussion

### *Eigen values*

Eigen values of PIOs express a contribution of the PIOs to the interaction. The eigen values of PIOs of each model are summarized in Table 1. Table 1 tells us that the eigen values of the  $\alpha$ -spin part and the  $\beta$ -spin part are almost the same, the main interaction is expressed in PIO-1, and the subsidiary interactions is expressed in PIO-2.

### *Contour maps*

Contour maps of PIO-1, PIO-2 of model**(10)** and **(14)** are shown in Fig. 4. We can visually understand in the both models that the PIO-1 expresses the electron

back-donation from the catalyst to the propylene and the PIO-2 expresses the electron donation from the propylene to the catalyst.

Table 1 The eigen values of PIOs of each model on the crystalline surfaces

Model	PIO-1		PIO-2		PIO-3		PIO-4		PIO-5		PIO-6		...	PIO-18	
	$\alpha$ spin	$\beta$ spin	$\alpha$ spin	$\beta$ spin	$\alpha$ spin	$\beta$ spin	$\alpha$ spin	$\beta$ spin	$\alpha$ spin	$\beta$ spin	$\alpha$ spin	$\beta$ spin		$\alpha$ spin	$\beta$ spin
(10)	<b>0.135</b>	<b>0.135</b>	<b>0.050</b>	<b>0.050</b>	0.036	0.031	0.027	0.023	0.019	0.015	0.014	0.013	...	0.000	0.000
(11)	<b>0.119</b>	<b>0.119</b>	<b>0.087</b>	<b>0.087</b>	0.040	0.041	0.030	0.030	0.017	0.017	0.011	0.011	...	0.000	0.000
(12)	<b>0.139</b>	<b>0.125</b>	<b>0.073</b>	<b>0.048</b>	0.034	0.031	0.023	0.023	0.015	0.015	0.012	0.012	...	0.000	0.000
(13)	<b>0.116</b>	<b>0.116</b>	<b>0.069</b>	<b>0.069</b>	0.032	0.032	0.020	0.020	0.014	0.011	0.010	0.010	...	0.000	0.000
(14)	<b>0.269</b>		<b>0.103</b>		0.067		0.048		0.032		0.029		...	0.000	
(15)	<b>0.128</b>	<b>0.128</b>	<b>0.056</b>	<b>0.056</b>	0.038	0.035	0.030	0.024	0.018	0.015	0.013	0.013	...	0.000	0.000
(16)	<b>0.128</b>	<b>0.128</b>	<b>0.054</b>	<b>0.056</b>	0.038	0.035	0.030	0.024	0.019	0.015	0.015	0.013	...	0.000	0.000

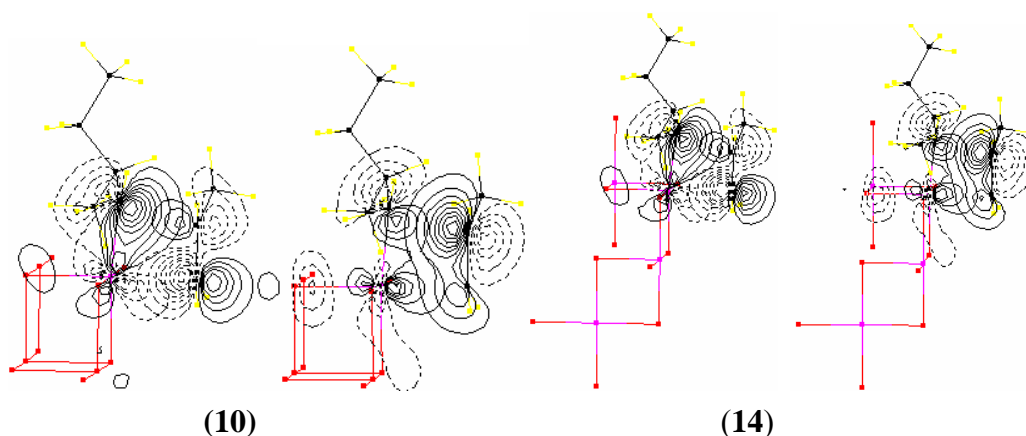


Fig. 4 Contour maps of  $\alpha$  spin of PIO-1 and -2 of model(10) and model(14).

### Overlap Populations

The overlap populations of the PIO-1 and PIO-2 of each model are summarized in Table 2. The larger the overlap population is, the larger the reactivity of the reaction is. According to the  $\Sigma$ OP of the PIO-1 and the PIO-2, we can estimate the order of the insertion activities as follows; **(11)** > **(13)** > **(16)**  $\geq$  **(15)** > **(14)** > **(10)** > **(12)**.

Followings are suggested; 1) the active sites having vacancy of trans to the propylene or the active sites having a weakly coordinated ligand trans to the propylene exhibit high insertion activity, 2) the activity of the Oh-MgCl<sub>2</sub> supported catalysts having a weakly coordinated donor trans to the propylene is markedly higher than that of TiCl<sub>3</sub> catalysts.

Table 2 The overlap populations (OP) of the PIO-1 and PIO-2 of each model

	PIO-1	PIO-2	$\Sigma OP(\alpha \text{ spin} + \beta \text{ spin})$ of PIO-1 and -2
(10) $\alpha$ spin	0.0338	0.0095	0.0922
$\beta$ spin	0.0336	0.0153	
(11) $\alpha$ spin	0.0712	0.1283	0.3989
$\beta$ spin	0.0712	0.1282	
(12) $\alpha$ spin	0.0351	-0.0438	0.0653
$\beta$ spin	0.0058	0.0682	
(13) $\alpha$ spin	0.0398	0.1106	0.3013
$\beta$ spin	0.0402	0.1107	
(14)	0.0617	0.0597	0.1214
(15) $\alpha$ spin	0.0428	0.0769	0.2405
$\beta$ spin	0.0429	0.0779	
(16) $\alpha$ spin	0.0473	0.0744	0.2454
$\beta$ spin	0.0474	0.0763	

## 5. CONCLUSION

An increasing of world demands of PP will be strongly continued. While the Gas phase polymerization process will keep a main tide of PP manufacturing processes, we have to always take care of effective consumption of raw materials and utilities for PP production. Several points will be focused on the future of the PP; 1) a change of chemical resources for propylene, 2) well designed copolymerization, 3) miscellaneous types of composites of PP with novel effective compatibilizers, 4) LCA of PP products.

## 6. ACKNOWLEDGEMENT

I would like to express my hearty thanks to Prof. Hiroshi Fujimoto for his kind guidance to execute PIO analysis and also express my gratitude to Sumitomo Chemical Co. Ltd..

## 7. APPENDIX

PIOs are obtained by applying the procedure that was proposed by Fujimoto et al. [22]. It is summarized as follows:

1) we expand the MOs of a complex in terms of the MOs of two fragment species, to determine the expansion coefficients  $c_{i,f}$ ,  $c_{m+j,f}$  and  $d_{k,f}$ ,  $d_{n+l,f}$  in Eq. 1;

$$\Phi_f = \sum_{i=1}^m c_{i,f} \phi_i + \sum_{j=1}^{M-m} c_{m+j,f} \phi_{m+j} + \sum_{k=1}^n d_{k,f} \psi_k + \sum_{l=1}^{N-n} d_{n+l,f} \psi_{n+l}, \quad (1)$$

$$f = 1, 2, \dots, m+n,$$

2) we construct an interaction matrix  $\mathbf{P}$  which represents the interaction between the MOs of the fragment [A] and the MOs of the fragment [B];

$$P = \begin{pmatrix} P_{i,k} & P_{i,n+l} \\ P_{m+j,k} & P_{m+j,n+l} \end{pmatrix} \quad (2)$$

in which

$$P_{i,k} = n_{i,u} \sum_{f=1}^{m+n} C_{i,f} d_{k,f} \quad i=1 \sim m, k=1 \sim n$$

$$P_{i,n+l} = n_{i,u} \sum_{f=1}^{m+n} C_{i,f} d_{n+l,f} \quad i=1 \sim m, l=1 \sim N-n$$

$$P_{m+j,k} = n_{m+j,u} \sum_{f=1}^{m+n} C_{m+j,f} d_{k,f} \quad j=1 \sim M-m, k=1 \sim n$$

$$P_{m+j,n+l} = n_{m+j,u} \sum_{f=1}^{m+n} C_{m+j,f} d_{n+l,f} \quad j=1 \sim M-m, l=1 \sim N-n$$

3) we obtain transformation matrix  $U^A$  (for A) and  $U^B$  (for B) by

$$\tilde{P} P U^A = U^A \Gamma \quad (3)$$

$$U_{s,v}^B = (\gamma_v)^{-1/2} \sum_r^N p_{r,v} U_{r,v}^A \quad v = 1, 2, \dots, N \quad (4),$$

4) and finally we obtain the PIOs by Eq. 5 and Eq. 6:

$$\phi'_v = \sum_r^N U_{r,v}^A \phi \quad (\text{for A}) \quad (5)$$

$$\psi'_v = \sum_s^N U_{s,v}^B \psi \quad (\text{for B}) \quad (6).$$

The  $N \times M$  ( $N < M$ ) orbital interactions in the complex C can thus be reduced to the interactions of N PIOs, N indicating the smaller of the numbers of MOs of the two fragments, A and B.

We used the extended Hückel parameters reported by G. Burns [24].

## References

- [1] K. Matsuyama, A. Shiga, M. Kakugo, and H. Hashimoto, *Hydrocarbon Processing*, **November 1980**, 131 (1980)
- [2] A. Shiga, *SHOKUBAI(CATALYST)*, **26**, 78 (1984); 1) JPN 32-987, 2) JPN 32-1545, 3) JPN 32-5746, 4) JPN 32-10596, 5) JPN 40-15982, 6) JPN 43-13050, 7) JPN 46-34078, 8) JPN 46-34092, 9) JPN 47-41676, 10) JPN 46-31330, 11) JPN 49-21433, 12) *JPAppl* 47-34478, 13) *JPAppl* 48-16986, 14) *JPAppl* 50-126590, 15) *JPAppl* 52-151691, 16) *JPAppl* 53-33289, 17) *JPAppl* 55-45722, 18) *JPAppl* 55-78004, 19) *JPAppl* 54-148093, 20) *JPAppl* 58-83006, 21) *JPAppl* 57-221659.
- [3] G. Natta, *J. Polymer Sci.*, **34**, 21 (1959)
- [4] G. Natta, P. Corradini and G. Allegra, *J. Polymer Sci.*, **51**, 399 (1961)
- [5] J. Boor Jr., "Ziegler-Natta Catalysts and Polymerization", Academic Press : New York, (1979)
- [6] T. Keii, "Kinetics of Ziegler-Natta Polymerization", Kodansha : Tokyo, (1972)
- [7] C. W. Hock, *J. Polymer Sci.*, **A-1, 4**, 3055 (1966)
- [8] a) J. Wristers, *J. Polymer Sci., Polymer Phys. Ad.*, **2**, 1601 (1973)  
b) J. Wristers, *J. Polymer Sci., Polymer Phys. Ad.*, **2**, 1619 (1973)

- [9] L. A. M. Rodoriguez and H. M. van Looy, *J. Polymer Sci.*, **A-1**, **4**, 1971 (1966)
- [10] M. Kakugo, H. Sadatoshi, M. Yokoyama and K. Kojima, "Transition metals and Organometallics as Catalysts for Olefin Polymerization", Springer-Verlag : Berlin Heidelberg 1988, p434
- [11] J. P. Luongo, *J. Appl. Polymer Sci.*, **3**, 302 (1960)
- [12] Y. Takegami, T. Suzuki and T. Okazaki, *Bull. Chem. Soc. Japan*, **42**, 1060 (1969)
- [13] T. Miyazawa and T. Ideguchi, *J. Polymer Sci.*, **B-1**, 389 (1963)
- [14] a) A. Zambelli, M. G. Gingo and G. Natta, *Makromol. Chem.*, **112**, 183 (1968)  
b) A. Zambelli and C. Tosi, *Adv. Polymer Sci.*, **15**, 32 (1974)
- [15] L. F. Johnson, F. Heatty and F. A. Bovey, *Macromolecules*, **3**, 175 (1970)
- [16] W. O. Crain, A. Zambelli and J. D. Roberts, *Macromolecules*, **4**, 330 (1971)
- [17] M. Kakugo, T. Miyatake, Y. Naito and K. Mizunuma, *Macromolecules*, **21**, 314 (1988)
- [18] Z. W. Wilchinsky, R. W. Looney and E. G. M. Tornqvist, *J. Catal.*, **28**, 354 (1973)
- [19] A. Shiga, J. Kojima, Y. Naito and T. Sasaki. *Polymer Preprints, Japan* **36**, 190, 191 (1987).
- [20] P. Cossee, *J. Catal.*, **3**, 80 (1964)
- [21] H. Kawamura-Kuribayashi, N. Koga and K. Morokuma, *J. Am. Chem. Soc.*, **114**, 2359 (1992)
- [22] H. Fujimoto, T. Yamasaki, H. Mizutani and N. Koga, *J. Am. Chem. Soc.*, **107**, 6175 (1985)
- [23] a) A. Shiga, H. Kawamura-Kuribayashi and T. sasaki, *J. Mol. Catal.*, **A98** 15 (1995) b) A. Shiga and M. Kubota, *Catalysis Letters*, 48, 89 (1997) c) A. Shiga, *J. Mol. Catal.*, **A146**, 325 (1999) d) A. Shiga, "Current Achievements on Heterogeneous Olefin Polymerization Catalysts" Sankeisha. Co. Ltd., Nagoya 2004, p255
- [24] G. Burns, *J. Chem. Phys.*, **41**, 1521 (1964)